.1

Part IV
Interstellar dust

Contents

.2

1 Extinction

Extinction

References:

Draine, B.T., 2003, "Astrophysics of Dust in Cold Clouds", astro-ph/0304488
Draine, B.T., 2004, ARA&A, 41, 241

- $A_\lambda \equiv -2.5\log_{10} I_{\rm obs}/I_{\rm int}$.
- $I_{\rm obs} = \exp(-\tau) I_{\rm int} \implies A_\lambda = 2.5\tau/\ln(10) \approx 1.086\tau(\lambda)$.
- A_λ is measured by comparing magnitudes for star with the same spectral type, or else using recombination lines.
- $R_V = A_V/E(B-V) = A_V/(B-V|_{\rm obs} - B-V|_{\rm int}) = A_V/(A_B - A_V)$

.3

Extinction

- grains $\ll \lambda$: Rayleigh-scattering gives $A_\lambda \propto \lambda^{-4}$, $R_V \approx 1.2$.
- grains $\gg \lambda$: gray extinction, independent of λ, $R_V \to \infty$.
- Parametrisation in terms of single parameter R_V OK for $\lambda > 3030$ Å:

$$A(\lambda), R_V) = a(\lambda) + b(\lambda)/R_V,$$

  where $a(\lambda)$ and $a(\lambda)$ are power laws, set by fitting the data (Cardelli et al., 1989, ApJ, 345, 245).
- For $\lambda < 3030$ Å , use $A_\lambda \approx f(\lambda; R_V, \{a_i\})$ where $\{a_i\}$ charasterise the UV 'bump'.
- In the IR, between 0.9 and 6μm, A_λ is $\pm$ universal: $A_\lambda = 2.4\ \lambda^{-1.75}$ (Draine 1989, quoting 'Infrared Astronomy', Tokunaga in *Astrophysical Quantities*).

.4

Extinction

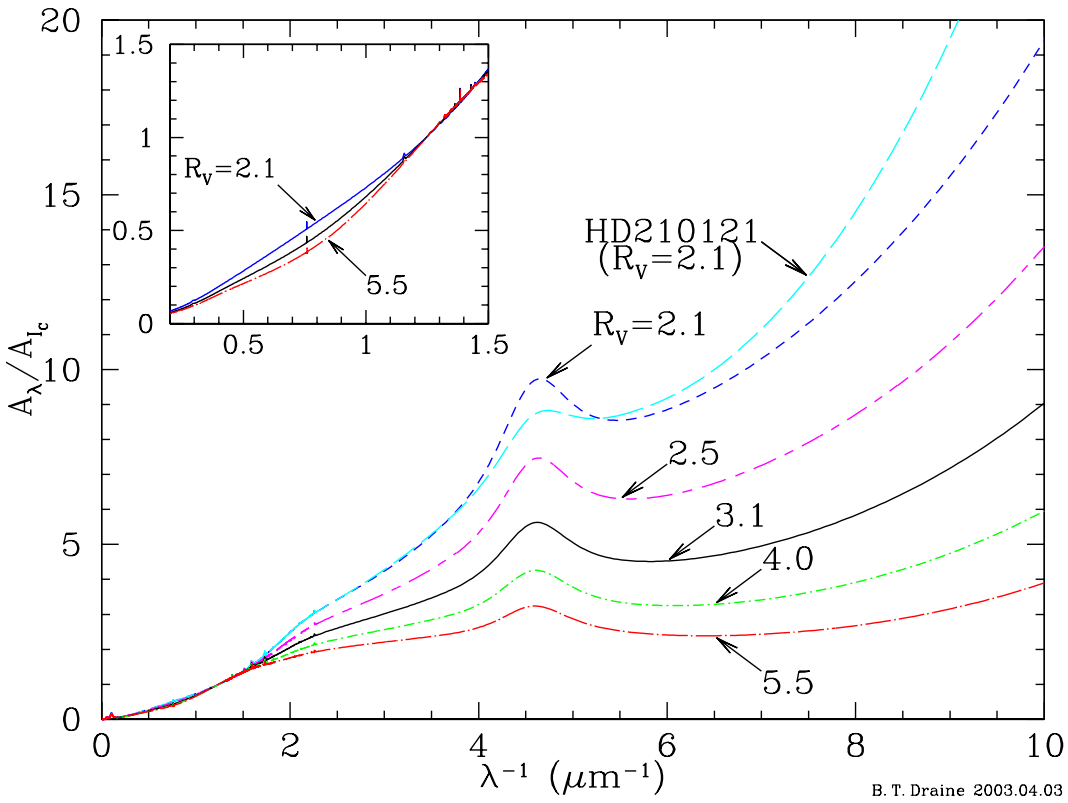

.5

Extinction

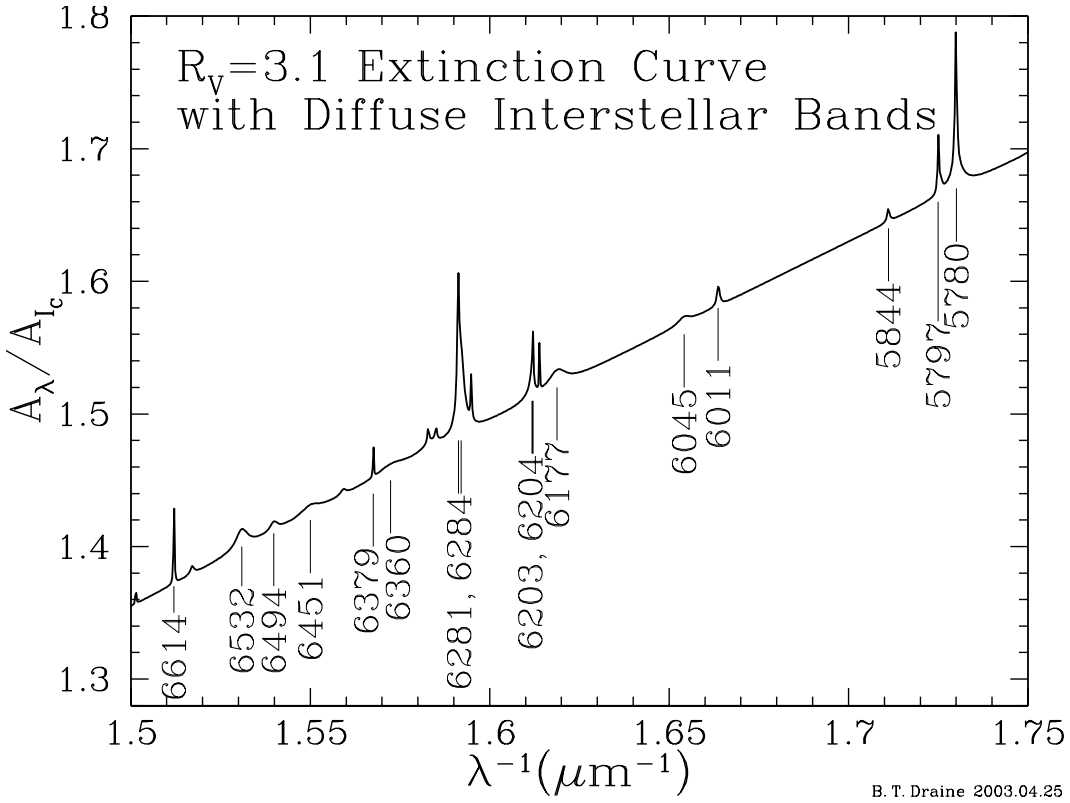

.6

R_V?

- Galactic bulge: $R_V = 1.8 - 2.5$ (Udalski 2002)
- LMC: $R_V = 3.1$ (Udalski 2002)
- Cirrus clouds (far from the galactic plane): $R_V = 2$ (Guhathakurta 1999).
- Typical value for the local ISM : $R_V = 3.1 \pm 2$!? (Cardelli et al 1989)

.7

$N_H \leftrightarrow A_V$[1]

Using H I Lyα and H_2 absorption lines to measure the column of protons to nearby stars gives $N_H/E(B-V) = 5.8\ 10^{21}$ cm^{-2}mag^{-1}, or $N_H/A_V = 1.87\ 10^{21}$ cm^{-2}mag^{-1}, for $R_V = 3.1$. But $N_H \leftrightarrow A_V$ varies with sighlines:

[1] ojo: A_V vs $1/R_V \propto 1/A_V$

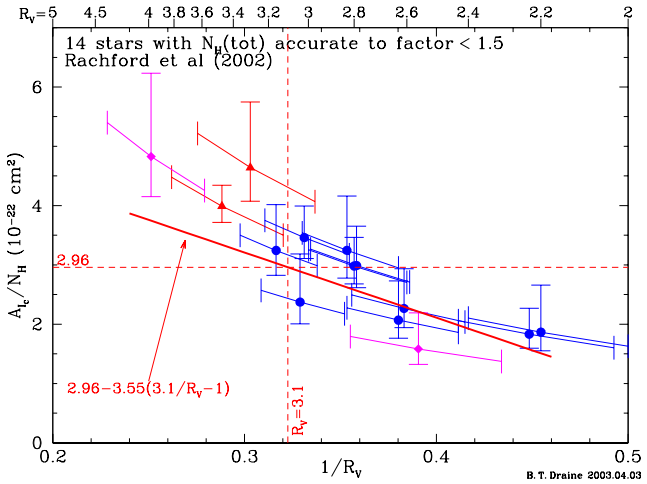

$A_V(N_H)$ follows Z in the Magellanic Clouds: 40% of Milky Way extinction in LMC, 10% in SMC.

.8

A_λ over 6-8 μm

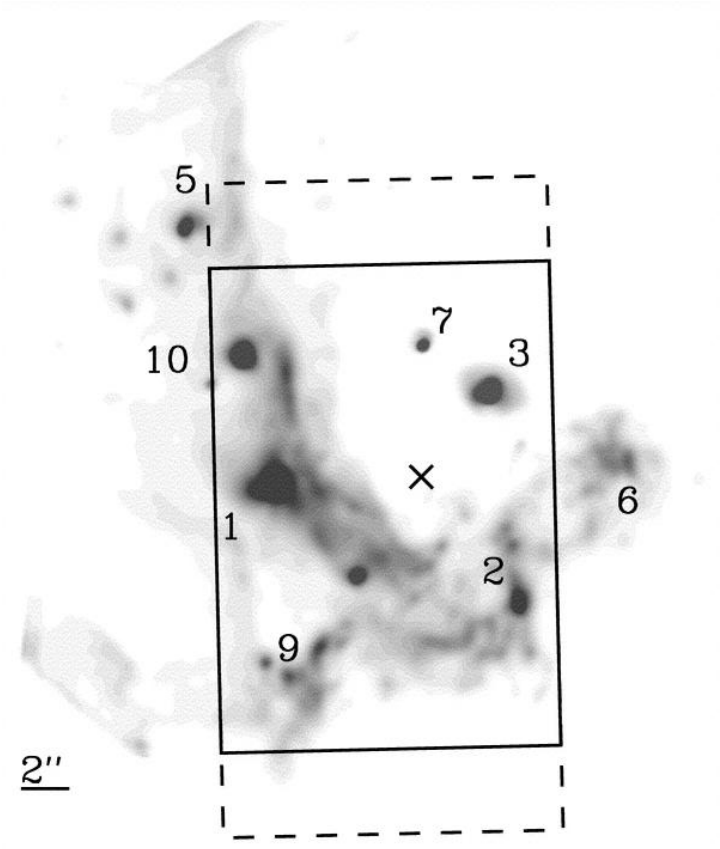

.9

A_λ over 6-8 μm

Lutz et al. (1996, A&A, 315, L269) find excess extinction assuming Case B for H recombination lines in the *ISO*+SWS spectrum.

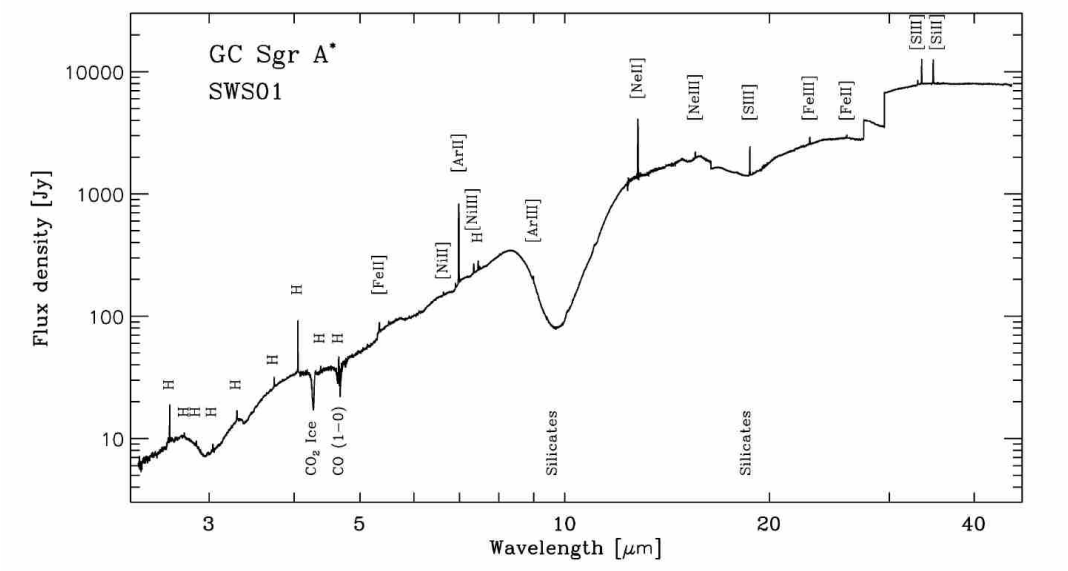

.10

A_λ over 6-8 μm

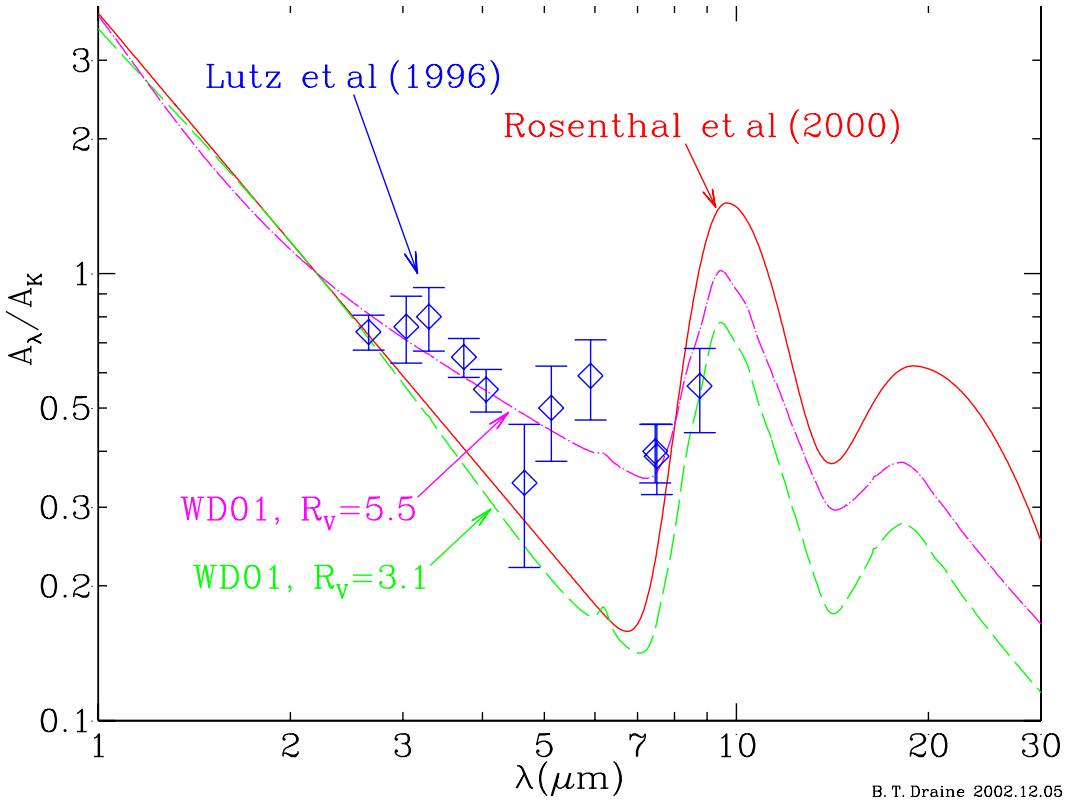

.11

Uncertainties in A_λ

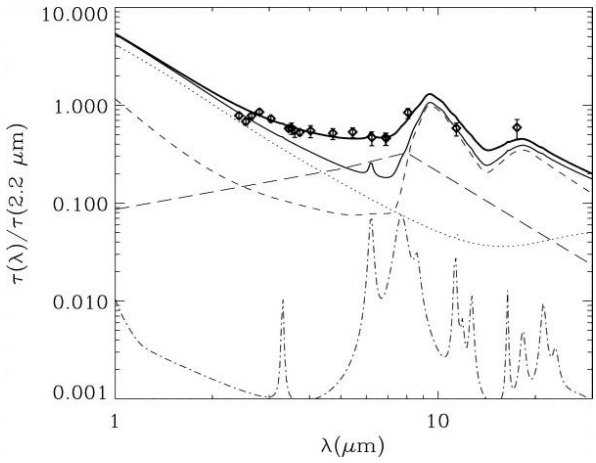

Dwek (2004, ApJL, 611, 109) proposes that the excess extinction at $\sim$6 μm is due to metallic needles (ref. Hoyle & Wickramasinghe). **short dash**: silicates, **long dash**: metallic needles, **dots**: graphite, **dot-dash**: PAHs, **thin solid**: standard extinction.

$$\tau(\lambda) = \sum_j \int_0^L ds \left[\int_{a_{\min,j}}^{a_{\max,j}} da f_j(a) \kappa_j(\lambda, a) \rho_{d,j}(a,s) \right], \text{ with}$$

$$\int_{a_{\min,j}}^{a_{\max,j}} f_j(a) = 1.$$

.12

NICER and A_V maps

Lombardi, Alves, 2001, A&A 377,1023.

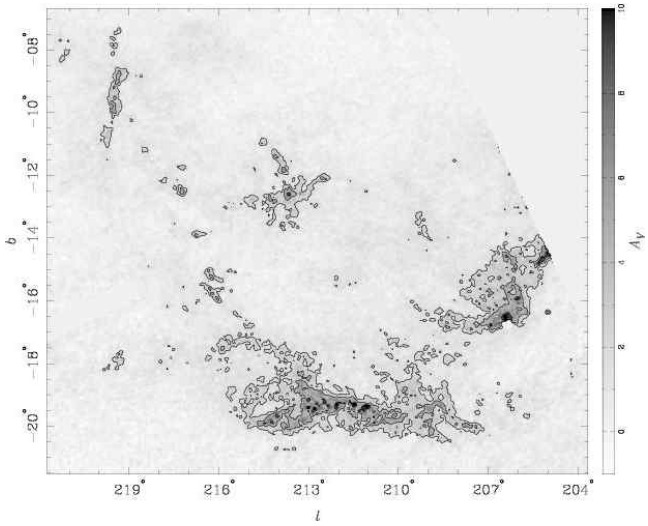

JHK extinction follows a fairly universal law, so JHK imaging allows accurate near-IR extinction measurements through stellar counts.

Very useful: A_V can be converted to N_H, and thereby to total masses.

.13

The UV bump: VSGs

- The UV bump matches a Lorentzian (in truth a 'Drude' profile).
- The fitting of a Lorentzian allows infering $n_X f_X / n_H = 9.3\ 10^{-6}$, and since the oscillator strength of the absorbing specie cannot be in excess of ~ 1, $f_X \lesssim 0.5$, one requires $n_X / n_H \gtrsim 4\ 10^{-5}$, allowing to consider compounds of $\{C, N, O, Mg, Si, Fe\}$.
- The centre of the bump is constant at 2175Å, although the width of the bump varies with $1\ \sigma \approx 6\%$.

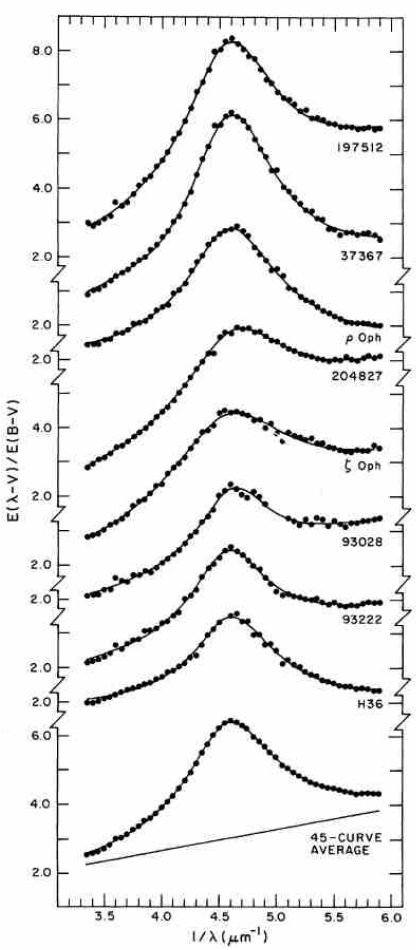

- A ground state transition in the delocalized electrons of the hexagonal benzene rings lies precisely at 2175Å.
- Graphite, with $f = 0.16$ could explain $\lambda_\circ$, and the absorption strength with C/H= $5.8\ 10^{-5}$ (OK for cosmic abundances), but not the FWHM variations.
- Variations in the mixture of different PAHs molecules are required to explain the $FWHM$ variations.

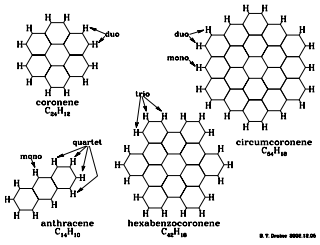

Silicate extinction

- The 10μm silicate feature is seen in absorption when the screen is colder than the background illuminating source. It is seen in emission in M stars (C/O$>$ 1) , or in planetary nebulae with C/O$>$ 1.
- Stretching mode of Si-O at 9.7 μm.
- Properties of silicates vary substantially with environment.

- The extinction curve at 10μm is smooth and shows no fine structure, in marked contrast with the crystalline silicate spectra $\Rightarrow$ interstellar silicates are amorphous.
- But there is a significant fraction of crystallinity in circumstellart disks and AGB (M) star outflows.
- Bowey et al. propose that up to 60% of silicate mass in dense dark cloud is crystalline (criticised).

.16

[2]

.17

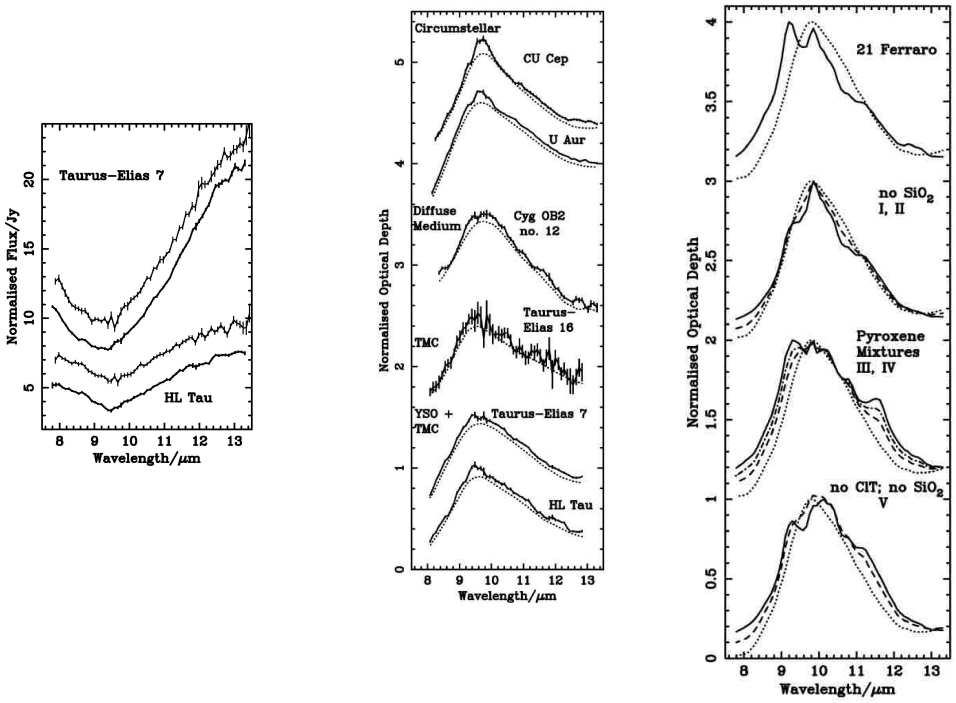

Silicate extinction

[2]Bowey & Adamson 2002, MNRAS, 334, 94

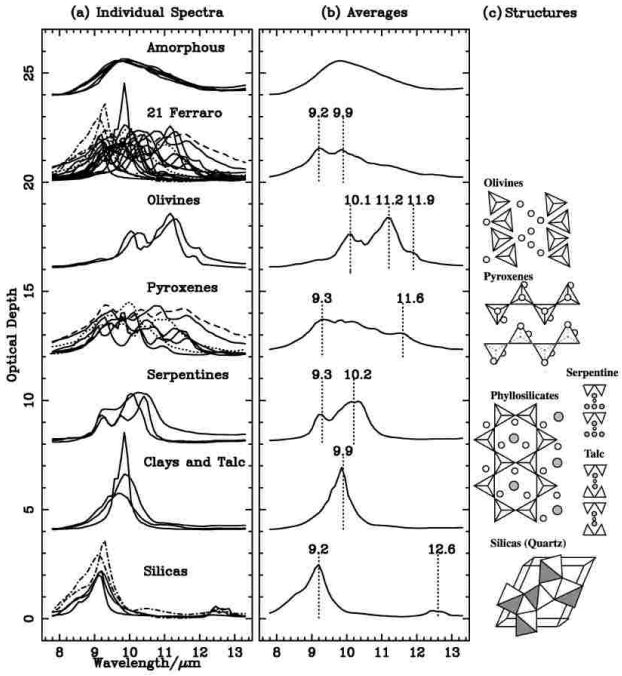

.18

Variations in the silicate profiles[3]

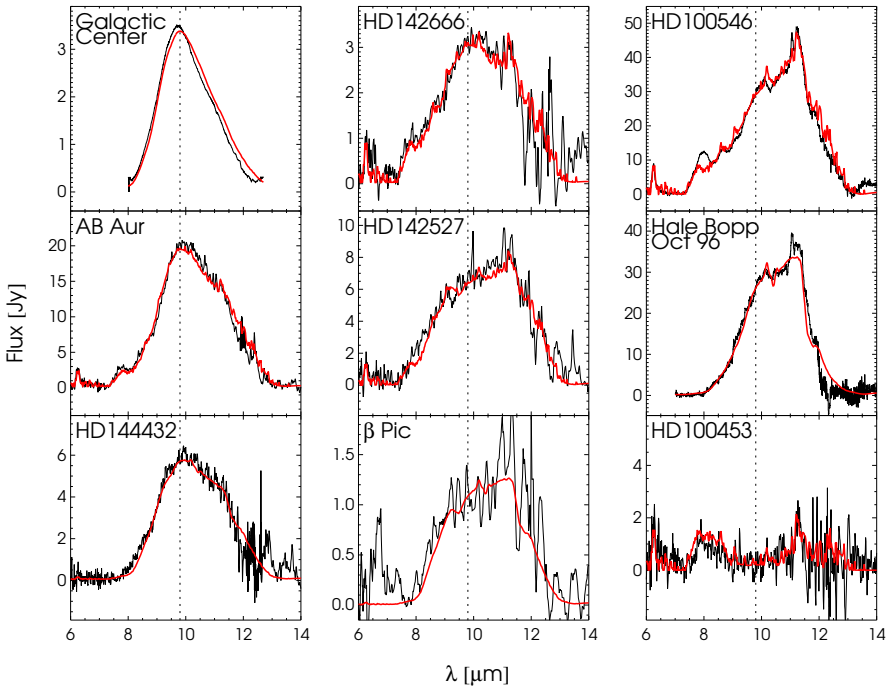

.19

[3]Van Dischoeck, 2004, AR&AA

Absence of crystalline silicates in the diffuse ISM[4]

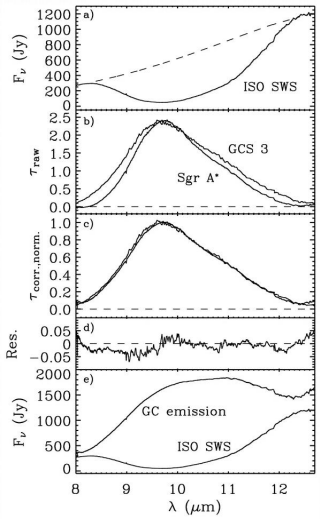

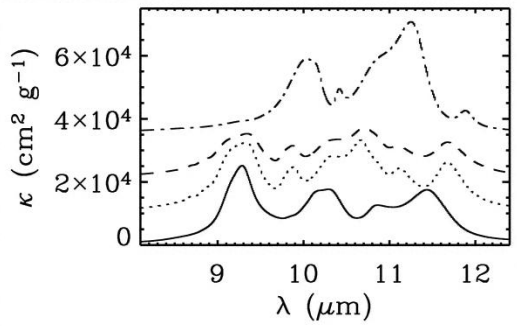

⇒ Crystalline silicates represent $\sim 0.2 \pm 0.2$ by mass.
Since the silicates in the AGB star outflows have high fractions of crystallinity, there must be substantial interstellar processing of dust in the ISM.

Ice absorption

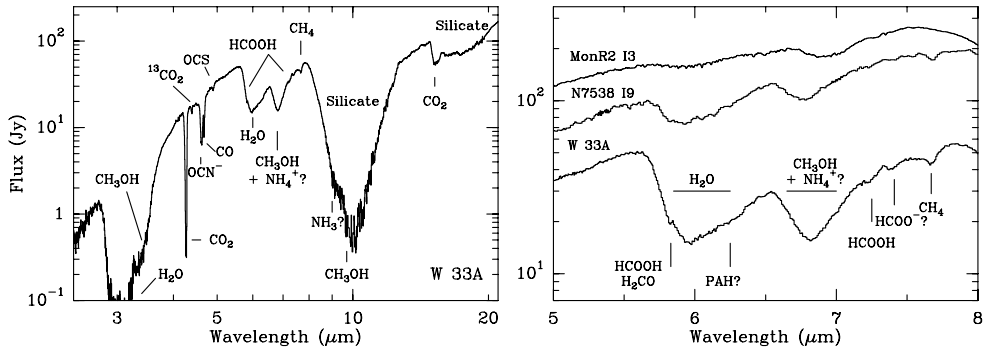

2 IR emission from dust

IR emission from dust

[4]Kemper et al. ApJ 2004, 609, 826

If the grains are in steady state, their internal energy and temperature are constant, and the emergent spectrum from a homogeneous cloud is

$$I_\nu = B_\nu(T_d)\,[1-\exp(-\tau_d)]\,,$$

with $\tau = \kappa(\lambda)\int \rho ds$, and

$$\kappa(\lambda) = \frac{1}{1.4 n_H m_H}\int da \frac{dn}{da} C_{\rm abs}(a,\lambda),$$

where ρ is the mass density (with gas), and $n(a)$ is the number density of grains with radii $< a$. Thus the column of mass is

$$\int \rho ds \approx \frac{1}{\kappa(\lambda)}\frac{I_\nu}{B_\nu(T_d)}\,.$$

The opacities κ and cross sections $C_{\rm abs}$ are tabulated in the web page of B. Draine: `http://www.astro.princeton.edu/~draine/dust/dust.html`. .22

IR emission from dust

The power absorbed by a grain is

$$\left.\frac{dE}{dt}\right|_{\rm abs} = \int_0^\infty d\nu u_\nu c C_{\rm abs}(\nu),$$

and emitted power is

$$\left.\frac{dE}{dt}\right|_{\rm rad} = \int_0^\infty d\nu 4\pi B_\nu C_{\rm abs}(\nu).$$

We can express T_s, the steady state temperature, from $\left.\frac{dE}{dt}\right|_{\rm abs} = \left.\frac{dE}{dt}\right|_{\rm rad}$, **under the assumption that collisions do not contribute to the thermal blance**.

But in reality E, the internal energy of the grain, and T, its temperature, vary stochastically, and the flutuactions are more pronouced when $h\nu \sim E$, as is the case for very small grains. .23

Feature at 3.4 μm: C-H alifatic stretch (carbon chains)

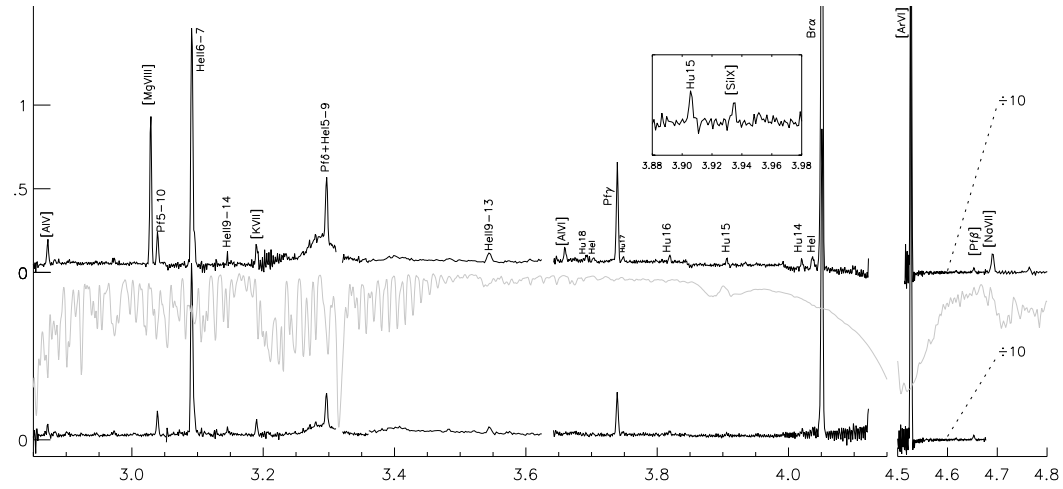

.24

Other dust features

- Diamonds are seen in two Herbig AeBe stars and one AGB star, through emission bands at 3.4 and 3.5 μm due to hydrogenated surface impurities on an otherwise regular carbon-crystal lattice.
- SiC (silicon carbide) is seen towards C stars and PNe.
- The Extended Red Emission, or a broad featureless continuum at 6000 to 8000 Å, is seen towards all lines of sight (i.e. cirrus and dark clouds, H II regions, PNe and galaxies in general). The carriers of ERE have yet to be identified.
- Fullerenes (Kroto et al. 1985, Nat, 318, 162) in post-AGB stars and PNe, e.g. Bernard-Salas et al., 2012, ApJ, 757, 41B

.25

3 VSGs

VSGs

- The VSGs are necessary to explain the variations in the UV bump of the extinction curve.
- Andriesse (1978) postulated the VSGs to explain the variation of the dust temperature in a cloud near M17. $T_{\rm colour}$ in the NIR and FIR are 150K y 38K, respectively, while the NIR and FIR morphologies are practically identical $\rightarrow$ the two temperatures are mixed, and it is necessary to postulate the temperature excursions of VSGs (which were called Platt particles at the time).
- Sellgren et al. (1983) found that the NIR emission in reflection nebula is extended and consists at least of one emission band at 3.3 μm as well as a continuum with $T_{\rm colour} = 1000$ K, with minimal variations with distance from the central star. Sellgren (1984, ApJ, 277, 623) noted that if the dust was in radiative equilibrium with the star, its temperature should decrease rapidly with distance, and so postulated the VSGs.

.26

VSGs

- The 12 μm and 25 μm emission from Galactic cirrus, discovered by *IRAS*, is much higher than that expected from large grains in equilibrium with the local radiation field (with T$\sim 18-25$ K, Boulanger & Perault 1988).
- Spinning dust?

.27

Stochastic heating of VSGs

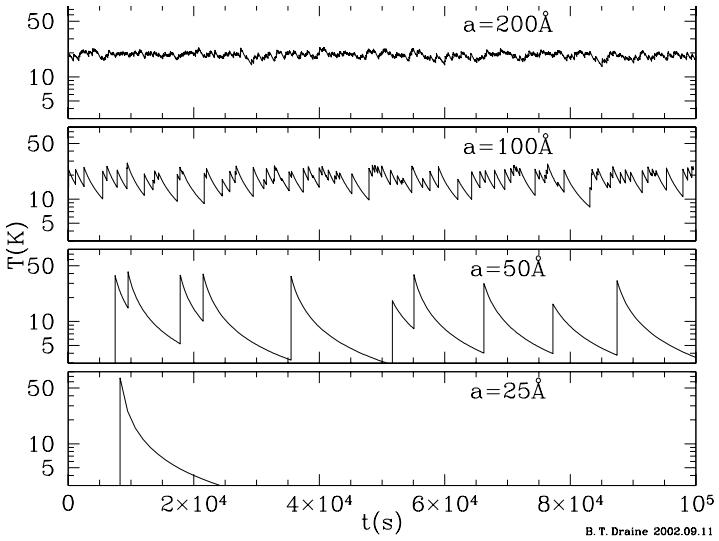

A grain with radius 5 Å(i.e. a PAH) receives 1 UV photon (10 eV) per year in the radiation field of the solar neighbourhood. When absorption occurs, the dust grain temperature may rise up to 1000 K. .28

.29

The state of the art in calculations of the VSG emissivity is that by Draine & Li (2001, ApJ, 551, 807), who estimated the quantized energy levels of the VSGs and their corresponding transition rates. See also Draine & Anderson (1985, 292, 494), Désert et al. (1986, A&A, 160, 295), Guhathakurtha & Draine (1989, ApJ, 345, 230).

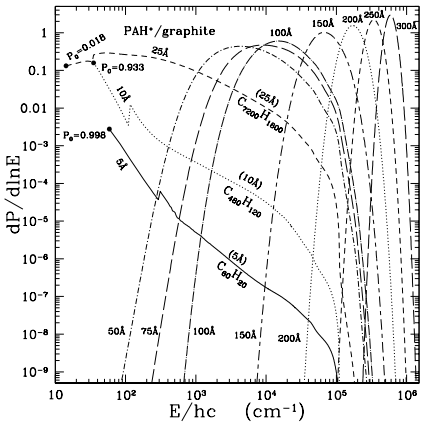

The problem involves modelling grains as discrete systems, where the rate of upwards transitions are

$$T_{l\to u} = C_{\rm abs}(E_u - E_l)c\frac{u_E}{E_u - E_l}\Delta E_u,$$

and $T_{u\to l}$ is obtained by detailed balance.

The probability density $P(E)$ in a discretized grain is then obtained by solving:

$$\frac{d}{dt}P_i = \sum_{j\neq i} T_{ij}P_j - \sum_{j\neq i} T_{ji}P_i.$$

Given $P(E)$, the power density emitted by a single grain is

$$S_\lambda = 4\pi \int dE \frac{dP}{dE} C_{\rm abs}(\lambda) B_\lambda(T(E)).$$

The temperature of the grain can be defined assuming the energy of the grain is equal to its expectation value, for a vibrational system in contact with a heat bath:

$$\langle E \rangle = \sum_j \frac{\hbar\omega_j}{\exp(\hbar\omega_j/kT) - 1},$$

where the sum extends over all normal modes. .30

It is reasonable to apply thermodynamics to a single molecule, say coronene ($C_{24}H_{12}$), because it has 10^{22} vibrational states with energies inferior to 1 eV $\Rightarrow$ $1/T = \partial S/\partial E$, in the canonical ensemble.

The function $P(E)$ depends on each astrophysical situation, but the only calculations available apply to the diffuse ISM. .31

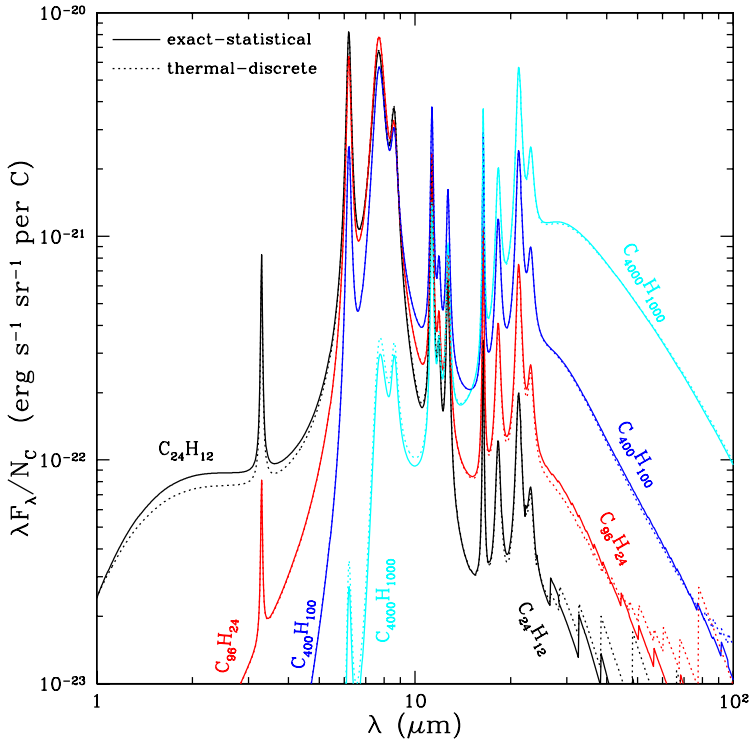

.32

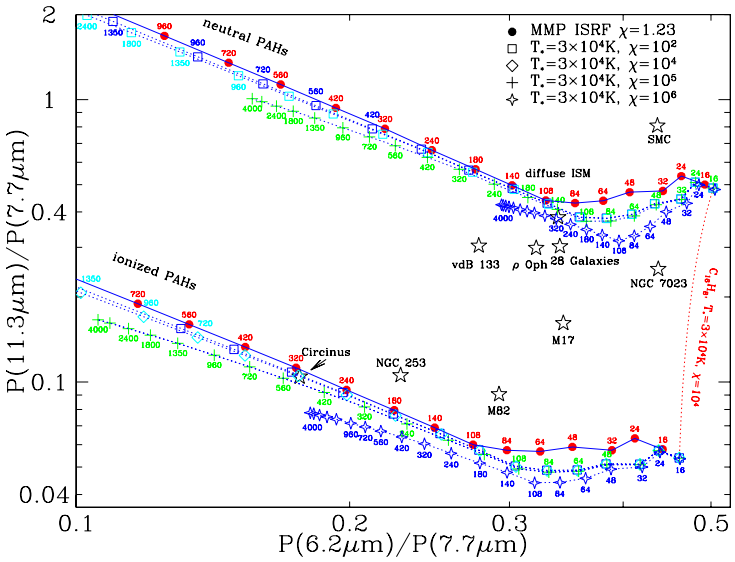

.33

4 The cycle of interstellar dust

Evolution of dust: sources

- dust features are observed in red giants.
- the "super-wind" on the AGB phase is very enriched in dust (AGB stars are conspicuous *IRAS* sources).
- M stars (with O/C $>$ 1 and classified by the presence of molecular lines such as TiO), show the silicate dust feature at 10μm.
- C stars (with C/O $>$ 1 and classified by the presence of molecular lines such as CH, C_2 y CN), show SiC features and graphite continuum.

The details of the condensation of dust are complex. It is believed that condensation occurs in "detashed shells" of the AGB phase (shielding from the stellar radiation is required to cool the shell and condense elements).

.34

Condensation temperatures

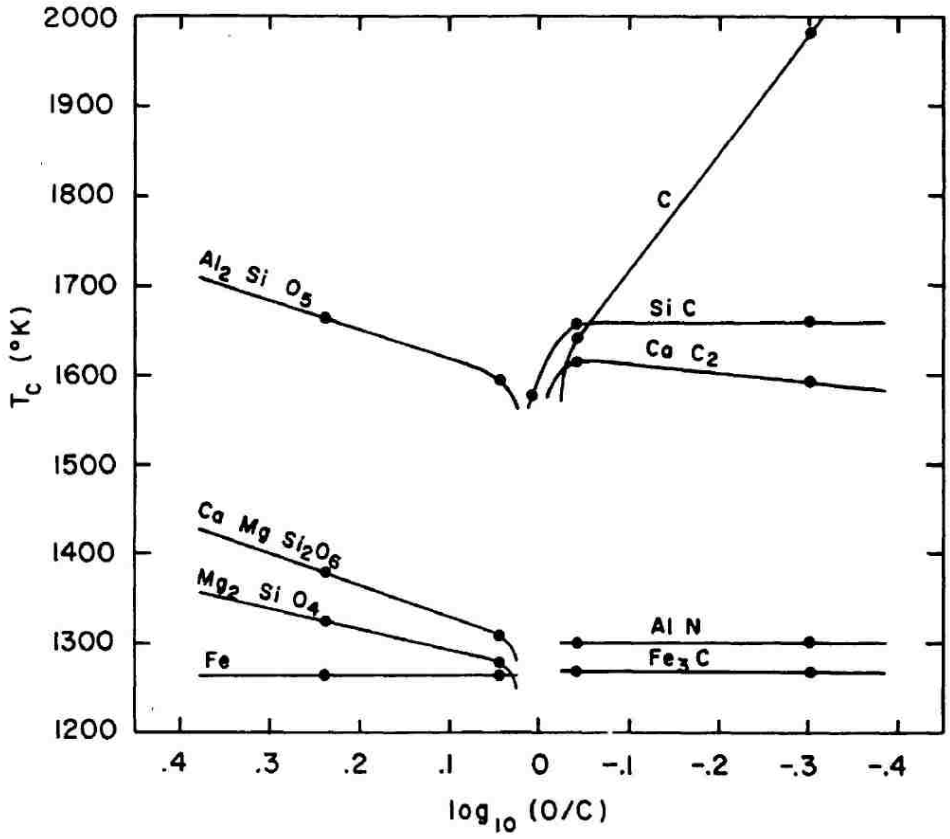

.35

Sources of interstellar dust

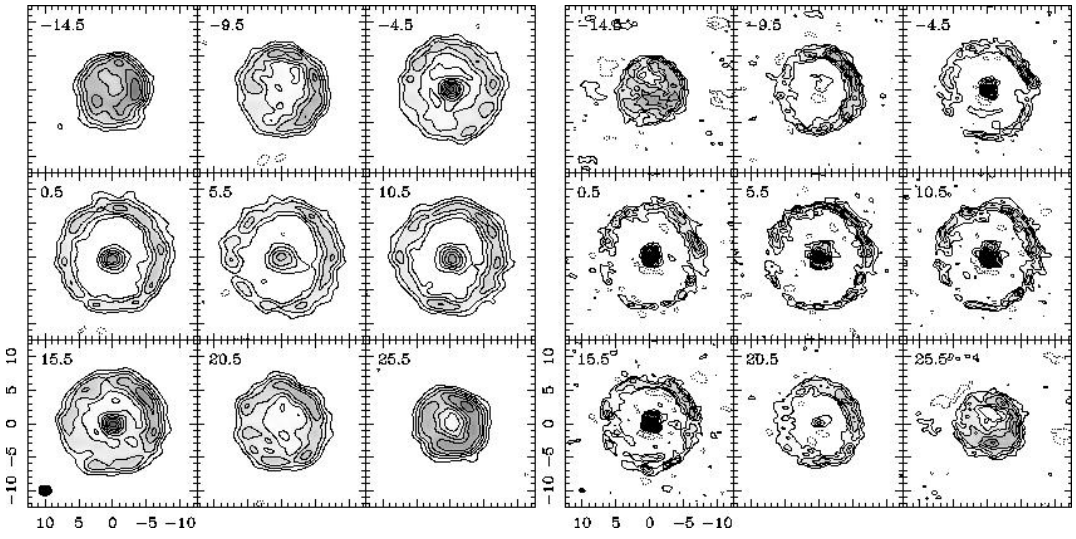

CO(1-0) and CO(2-1) in UCameopardalis (Lindqvist et al. 1998, 351, L1) → He-shell flashes modulate the rate of mass loss from $\sim 10^{-7} M_\odot$ yr^{-1} to $\sim 10^{-5} M_\odot$ yr^{-1}.

.36

AGB stars

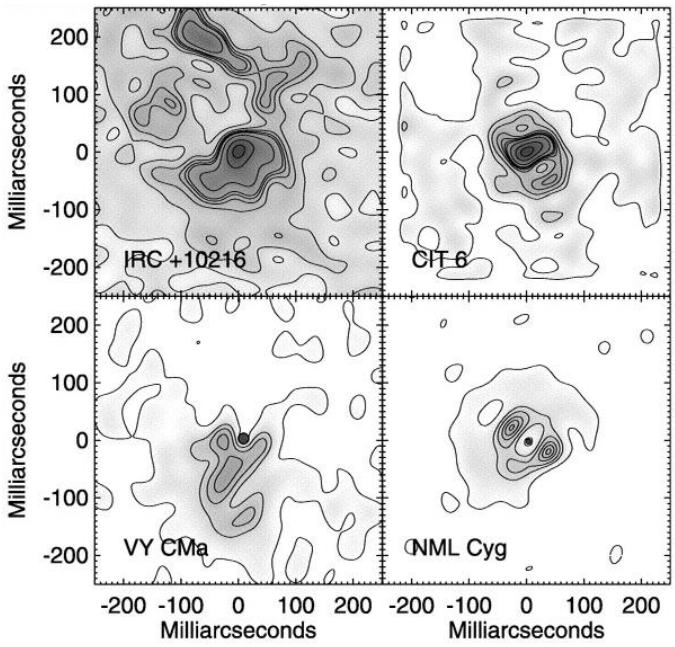

Monnier et al. (2004, ApJ, 605, 436). .37

Evolution of dust: IRC+10216

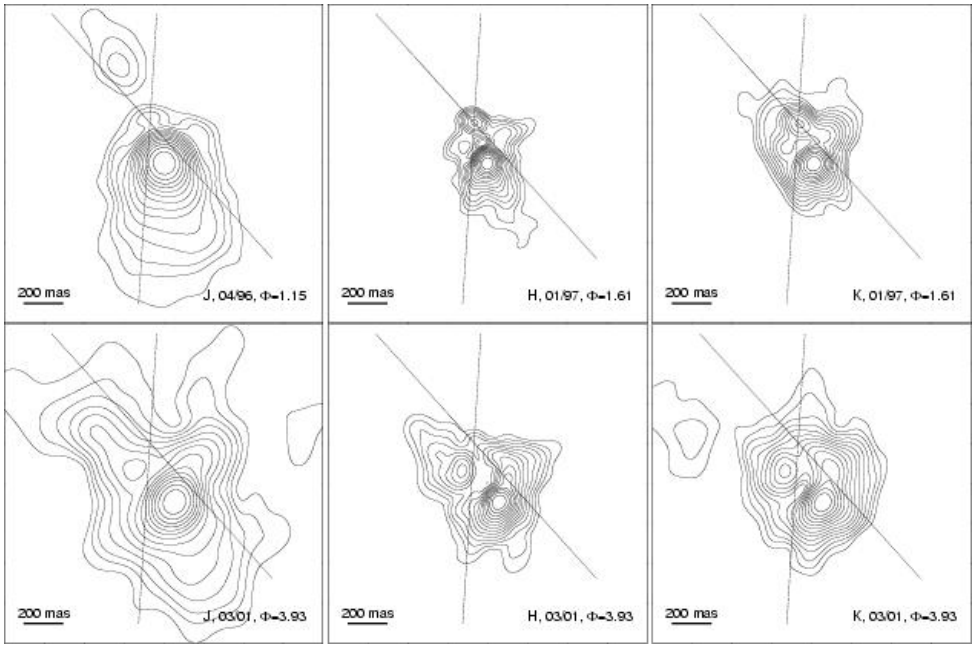

Time evolution of the dusty envelope (Weigelt et al. 2002, A&A,392, 131). .38

Evolution of dust: the PN phase

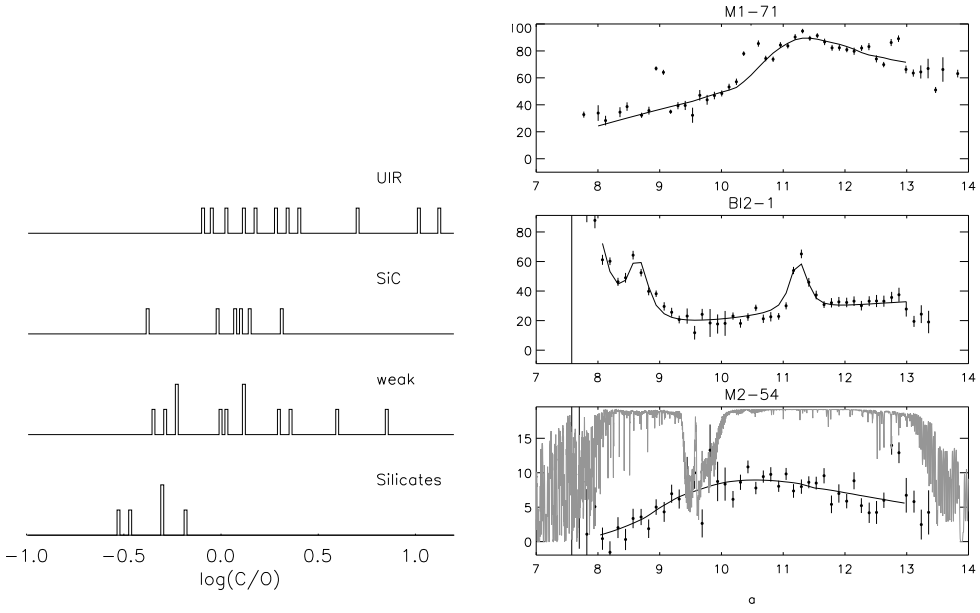

.39

Evolution of dust: the PN phase and the C/O dichotomy

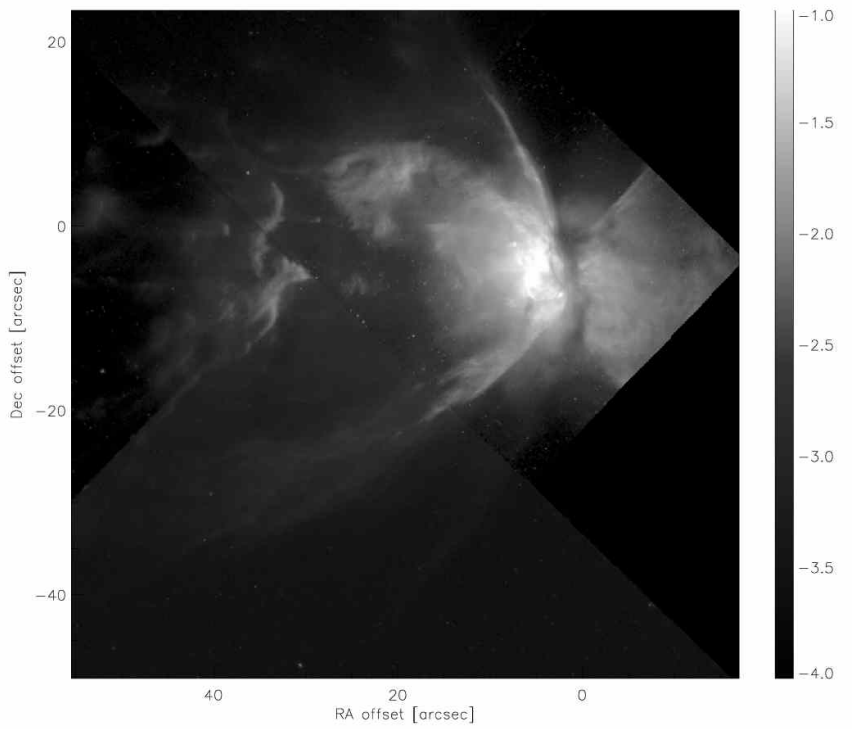

.40

Evolution of dust: the PN phase and the C/O dichotomy

18um silicates 11.3um PAH 11.3/18

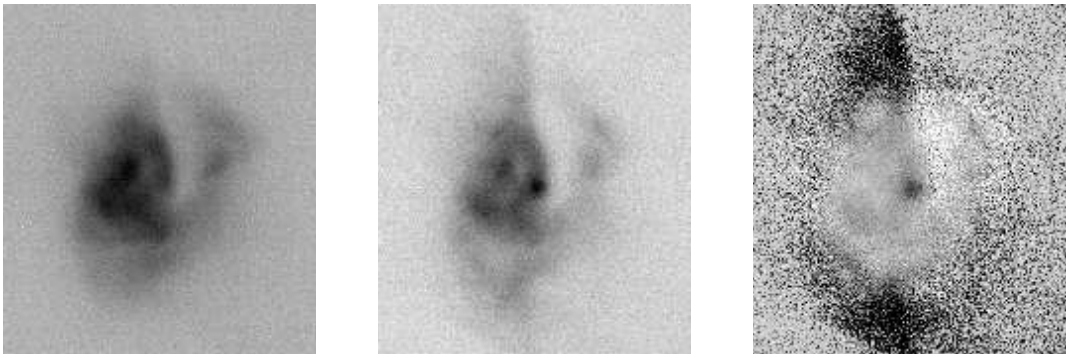

.41

Evolution of dust: SNe as dust factories

- Red giants and supergiants are easily indentified as sources of interstellar dust. Evolved stars inject dust in the ISM. But does circumstellar dust survive the SN event?
- The sub-mm detection of red-shifted dust from primordial galaxies (Ivison et al. 2000, MNRAS, 315, 209) implies the efficient production of dust on very short timescales, such as can only be provided by type II SNe.
- Isotopic anomalies in meteoritic inclusions favor the production of dust following the SN event (i.e. the SUperNOvaeCONdensates).
- The thermal echo due to radiative heating of the dusty winds from the precursor star (as in SN 1987A, Roche 1989, Nature, 337, 533) allows a measure of the circumstellar dust mass, and thereby a constraint on the precursor spectral type. Such a diagnostic is a lot more difficult from the near-IR spectra (uncertain contribution from VSGs and other excitation mechanisms).

.

.42

SN 1987A

Bouchet et al. (2004, ApJ, 611, 394) found a mid-IR source in SN 1987A, at the location of the SN ejecta, with about 10^{-3} $M_{\odot}$ in dust.

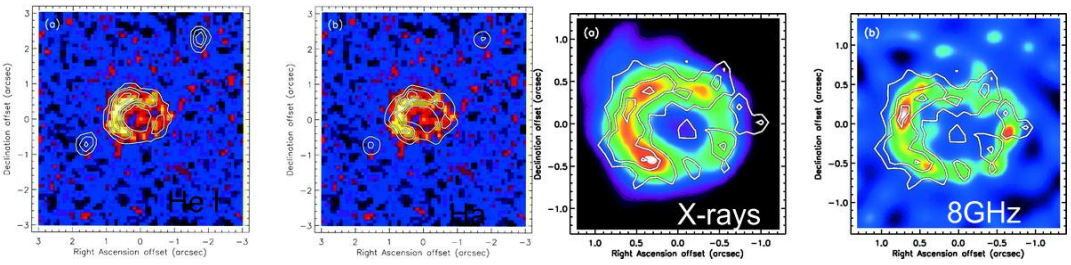

.43

SN 1987A

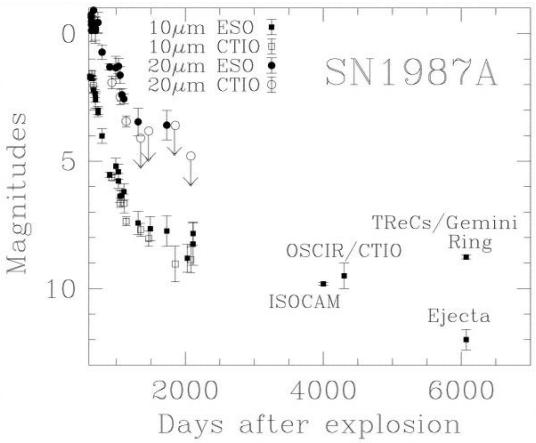

The ejecta detected by Bouchet et al. corresponds to the exponentially decaying mid-IR lightcurve. The equatorial ring is currently heated by the collision of the supernova blast on circumstellar shell.

.44

SN 2002hh: first IR echo since SN 1987A.

.45

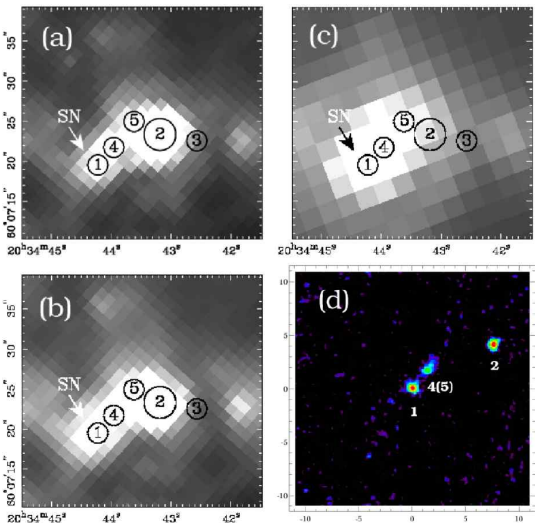

- (a, b) SINGS IRAC 5.8 and 8.0 μm images of a 30"x29" region around SN 2002hh (1.1" per pixel), obtained on 2004 June 10.
- (c) SINGS MIPS 24μm image of the same region (2.6" per pixel), obtained on 2004 July 9.
- (d) Gemini North Michelle 11.2μm image of SN 2002hh (0.099"), obtained on 2004 September 26.

SN 2002hh: first IR echo since SN 1987A.

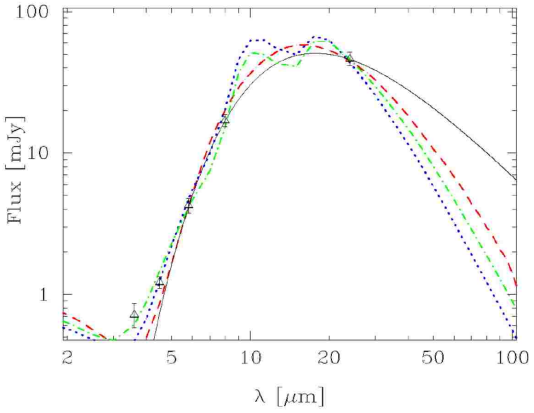

The modelling of the radiatively heated dust in SN 2002hh yields a total dust mass of 0.10–0.15 $M_\odot$, giving a progenitor mass of ∼10–15 $M_\odot$. The parameters of the dust shell are reminiscent of those around Galactic LBVs: a radius of 0.5–1 pc, dust masses of 0.1–0.3 $M_\odot$. .46

SN 2002hh.

- The IR luminosity of SN 2002hh at day 600 is $\sim 10^7 L_\odot$, much higher than that expected for the SN ejecta.
- Hence the observed mid-IR emission is due to flash-heated dust, a kind of "thermal echo".
- The thermal echo interpretation, rather than the condensation of dust in the SN ejecta, is also supported by the absence of line asymmetries in SN 2002hh for the same epoch (Clayton & Welsh 2004, AAS meeting).
- By comparison, SN 1987A scaled to the distance of SN 2002hh would have a factor of 35 less mid-IR flux at the same epoch.

.47

Dust condensation and emission line asymmetry.

- Among the discoveries in SN 1987A, oberved around day 600 but largely unexploited, is the asymmetry of optical emission lines generated by dust internal to the ejecta (Danziger et al. 1989, IAUC 4746). Dust condenses during the cooling related to the violent expansion, after day $\sim$ 300. Dust absorption extinguishes the red-shifted side of the metal-rich ejecta, thereby blue-shifting the obserbed profiles. Scattering off dust in an expanding nebula should also generate a red tail in the emission line profiles.

.48

Dust condensation in Cas A.

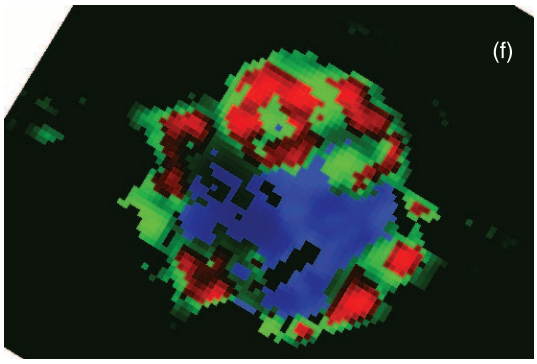

Rho et al. 2008.

.49

Evolution of dust: Condensation in hostile environments

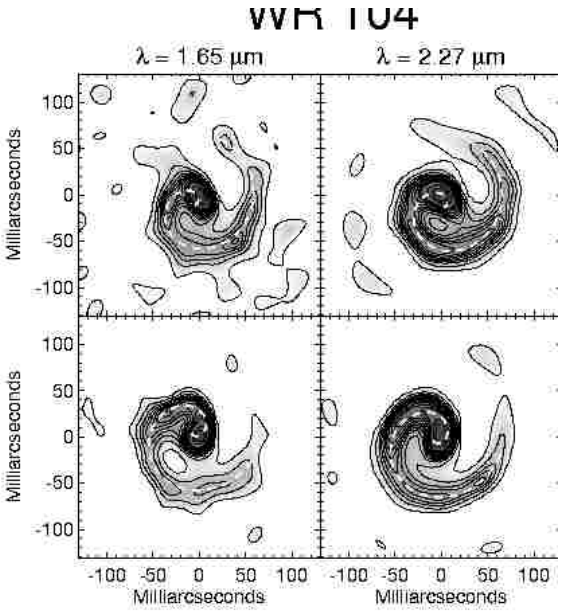

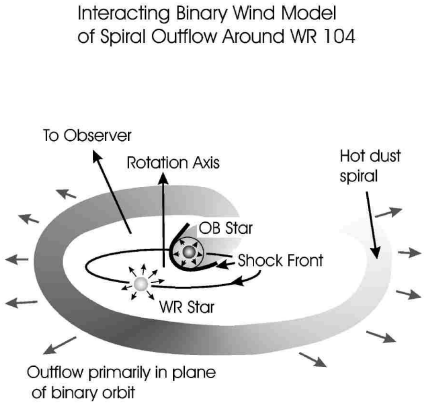

.50

Evolution of dust: survival in ionised regions

- The refractory elements (with high condensation temperatures) are systematically underabundant in H II regions, even in the presence of intense X-ray fields (Aller et al. 1981, Pwa et al., 1984, 1986, Oliva et al. 1996, Kingdon & Ferland 1997, Casassus et al. 2000).
- There is an IR excess in the direction of H II regions (Spitzer 1978).
- Ercolano et al. (2003, MNRAS, 344, 1145) show it is necessary to include the photoelectric effect in order to raise the temperature of regions with supersolar metallicity (in particular in the models with dual chemistries required to explain the ORL/CEL discrepancy).

.51

Evolution of dust: destruction of dust and time scales[5]

- Presolar grains in meteorites (e.g. in Murchison) show isotopic anomalies associated to stardust. But this does not imply that the bulk of the dust in the ISM is indeed stardust.
- ISM dust is destroyed in SN shock waves (Tielens et al. 1994, ApJ, 431, 321), by sputtering from heavy ions in hot gas, by grain-grain collisions leading to grain vaporization and fragmentation, and by UV exposure, which depletes the VSGs.
- *Models* of the evolution of dust grains for the various phases of the ISM *show* that the time scale for the residence of one atom in a given grain is $\tau_{\rm dest} \sim 3\,10^8$ yr.
- The rate of star formation in our Galaxy is $dM/dt \sim 5$ M$_\odot$ yr^{-1}, and the total mass of the ISM is $M_{\rm ism} \sim 5\ 10^9$M$_\odot$. The time scale for the residence of refractory elements in the ISM is thus $\tau_{\rm ism} \approx M_{\rm ism}/dMdt \approx 10^9$.

.52

Evolution of dust: destruction of dust and time scales

- Therefore the fraction of τ_{ism} that a given element spends inside a grain is $\tau_{\rm dest}/\tau_{\rm dest} + \tau_{\rm ism} = 0.2$ (why not $\tau_{\rm dest}/\tau_{\rm ism}$?). $\rightarrow$ if no dust is produced in the ISM, then 20% of the refractory elements should be locked in dust.
- But the prediction that 20% of the refractory elements are in dust does not match observations, which give up to 90% for Si $\rightarrow$ dust is produced in the ISM
- The mass of the Milky Way ISM is uncertain to 1 order of magnitude, and so is the rate of star formation, and therefore the fraction of Si in grains.

.53

[5]Draine, B.T., 2004, ARA&A, 41, 241